1977-06

Ballistic damage of graphite-epoxy plates

Eaton, George Arthur

NAVAL POSTGRADUATE SCHOOL
Monterey, California

THESIS

BALLISTIC DAMAGE OF GRAPHITE-EPOXY PLATES

by

George Arthur Eaton

June 1977

Thesis Advisor: M. H. Bank

Approved for public release; distribution unlimited.

NAVAL POSTGRADUATE SCHOOL
Monterey, California

THESIS

BALLISTIC DAMAGE OF GRAPHITE-EPOXY PLATES

by

George Arthur Eaton

June 1977

Thesis Advisor: M. H. Bank

SECURITY CLASSIFICATION OF THIS PAGE (When Data Entered)

REPORT DOCUMENTATION PAGE		READ INSTRUCTIONS BEFORE COMPLETING FORM
1. REPORT NUMBER	2. GOVT ACCESSION NO.	3. RECIPIENT'S CATALOG NUMBER
4. TITLE (and Subtitle) Ballistic Damage of Graphite-Epoxy Plates		5. TYPE OF REPORT & PERIOD COVERED Master's Thesis; June 1977 6. PERFORMING ORG. REPORT NUMBER
7. AUTHOR(s) George Arthur Eaton		8. CONTRACT OR GRANT NUMBER(s)
9. PERFORMING ORGANIZATION NAME AND ADDRESS Naval Postgraduate School Monterey, California 93940		10. PROGRAM ELEMENT, PROJECT, TASK AREA & WORK UNIT NUMBERS
11. CONTROLLING OFFICE NAME AND ADDRESS Naval Postgraduate School Monterey, California 93940		12. REPORT DATE June 1977 13. NUMBER OF PAGES 62
14. MONITORING AGENCY NAME & ADDRESS(if different from Controlling Office)		15. SECURITY CLASS. (of this report) Unclassified 15a. DECLASSIFICATION/DOWNGRADING SCHEDULE

16. DISTRIBUTION STATEMENT (of this Report)

Approved for public release; distribution unlimited.

17. DISTRIBUTION STATEMENT (of the abstract entered in Block 20, if different from Report)

18. SUPPLEMENTARY NOTES

19. KEY WORDS (Continue on reverse side if necessary and identify by block number)

20. ABSTRACT (Continue on reverse side if necessary and identify by block number)

Thin eight-ply laminated graphite-epoxy plates of a representative lay-up $(0/\pm 45°/0)_s$ were damaged ballistically. The extent of damage varied with impact velocity and impactor mass. Visual and microscopic inspection was augmented by x-ray inspection utilizing a radio-opaque dye, to evaluate the extent of damage area. Specimens were then tested in tension to failure, to evaluate the residual strength. Damage "length" (in the 0°

DD FORM 1 JAN 73 1473 EDITION OF 1 NOV 65 IS OBSOLETE
S/N 0102-014-6601

Approved for public release; distribution unlimited.

Ballistic Damage of Graphite-Epoxy Plates

by

George Arthur Eaton
Lieutenant Commander, United States Navy
B. S., United States Naval Academy, 1965

Submitted in partial fulfillment of the
requirements for the degree of

MASTER OF SCIENCE IN AERONAUTICAL ENGINEERING

from the

NAVAL POSTGRADUATE SCHOOL

June 1977

Author [redacted]

Approved by: [redacted]
Thesis Advisor

[redacted]
Chairman, Department of Aeronautics

[redacted]
Dean of Science and Engineering

ABSTRACT

Thin eight-ply laminated graphite-epoxy plates of a representative lay-up $(0/\pm 45°/0)_s$ were damaged ballistically. The extent of damage varied with impact velocity and impactor mass. Visual and microscopic inspection was augmented by x-ray inspection utilizing a radio-opaque dye, to evaluate the extent of damage area. Specimens were then tested in tension to failure, to evaluate the residual strength. Damage "length" (in the 0° direction) varied with impact velocity, the greatest damage resulting from the lower velocities. Damage "width" (in the 90° direction) was not greatly affected by velocity changes. Variation of impactor mass had little effect. Residual strength as measured by tensile tests in the 0° direction was insensitive to damage size effects.

TABLE OF CONTENTS

LIST OF FIGURES

I. INTRODUCTION

Advanced laminated composite materials are finding increasing areas of application in structures. Where high stiffness and high strength-to-weight ratios are necessary, such as in the case of aircraft construction, laminated composites meet the need and offer potential savings in structural weight estimated between 15% and 30%. Of course, these weight savings translate into higher performance for fighters, greater payload for bombers and transports, and more range and on-station time for anti-submarine warfare and surveillance aircraft.

As the weight savings resulting from composite use have been shown, and as confidence in design and manufacturing technology has grown, the use of composites in aircraft, especially military aircraft, has increased dramatically. The F-111 had a composite speed-brake. Composite leading edge flaps were tested on the C-5A. The F-14 production horizontal stabilizers have composite skins, and the entire empennage of the YF-16 uses composite skins. The F-18 wing will use graphite-epoxy laminate composite skins, with thicknesses at the root of 0.9 inches.

Any military aircraft may be subjected to a hostile environment. Even transport or surveillance aircraft may be called upon to brave hostile fire, and in doing so may sustain ballistic damage. Thus it is important to the designer to know the effects of ballistic damage on the

material that he intends to use in a military aircraft. A great body of information has grown up over the years on the ballistic response of conventional materials such as aluminum. Considerably less information is available on the ballistic response of advanced laminated composite materials.

In addition, if because of proper use of material and good design a composite-material aircraft survives ballistic damage, the immediate questions asked will be, "can the damage be repaired? What size patch will be required?" To answer these questions the size of the damaged areas must be known. And since composite laminates may delaminate under impact, the extent of the damaged area may not be obvious.

In an effort to develop an appreciation of the damage caused by ballistic impact on advanced laminated composite materials, especially when used as aircraft skins, the program reported in this thesis was undertaken. In brief, thin plates of a balanced symmetric lay-up $(0/\pm 45°/0)_s$ were manufactured, damaged on the ballistic range, inspected, and finally tested to determine their residual strength. Undamaged specimens and specimens with drilled holes were used as controls.

II. OUTLINE OF THE TEST PROGRAM

Since the majority of the vulnerable area of an aircraft exposed to a ballistic threat is at least covered by a "skin" panel, and since skins in semi-monocoque aircraft structures are load-carrying members of the structure, it was decided to investigate the effect of ballistic impact on a flat composite panel, representative of thin aircraft skins. The panel lay-up chosen was $(0/\pm 45°/0)_s$, i.e., first a lamina with fibers oriented in the zero direction, on top of that a lamina with fibers oriented 45° clockwise to the zero direction, then a lamina with fibers oriented 45° counter-clockwise to the zero direction, and another zero-direction lamina. This four-ply sequence was then mirrored, to make up the eight-ply symmetric laminate specified. This laminate is both "balanced" (has a $-\theta°$ ply for every $+\theta°$ ply) and "symmetric" ($+\theta°$ plies come in pairs located symmetrically, "n" layers above and below the laminate midplane). As a result, normal stress is independent of shear strain and shear stress is independent of normal strain, and there is no coupling between extension and bending.

Although it might seem advantageous in many applications to orient the reinforcing fibers in a laminated composite in the principal stress directions, that is seldom done. There are several reasons for this fact. First is the difficulty in predicting loads, and the necessity to be prepared for unexpected loads. These considerations dictate

that strength and stiffness be provided in directions other than the predicted principal directions. Perhaps more important is the difficulty in analyzing, optimizing, and manufacturing a laminated part in which lamina orientations are free to assume any value. Current practice, then, is to design the best laminate possible, using 0°, $\pm$45°, and 90° lamina orientations, only. The percentage of plies in each of these directions is adjusted to give the desired laminate performance. Since a wing skin is stressed mainly in tension/compression and torsion, the orientation code chosen, $(0/\pm 45°/0)_s$, is a good candidate for a wing skin material.

The experimental program undertaken was aimed at finding a way to determine the extent of damage to an aircraft skin which is caused by ballistic impact. Two factors seemed to be of primary importance: first, what is the physical size of the damaged area? How can the skin be inspected easily to determine damage size? Can the size be related to projectile parameters? And second, how much does the damage reduce the load-carrying capability of the skin panel?

To answer these questions, the experimental program proceeded in three test series:

A. TEST SERIES 1 - SEVEN SPECIMENS

In the first series, seven specimens were subjected to ballistic impact at velocities which varied from 1000 to 4000 feet per second in increments of 500 feet per second. Mass and diameter of the impacting projectile remained

constant. Each of the specimens was then examined using four different candidate inspection techniques: visual, ultrasonic, x-ray, and microscopic.

B. TEST SERIES 2 - THREE SPECIMENS

In the second test series three additional specimens were damaged ballistically. For these tests the projectile velocity was held constant, as was the diameter, but the masses were varied. Projectile weights of 27.5, 45, and 63 grains were used. The specimens were then examined and damage size determined visually and with an improved x-ray inspection.

C. TEST SERIES 3 - TWENTY-ONE SPECIMENS

The third test series involved fifteen specimens which were ballistically damaged, and six control specimens. Ballistic impact velocity was varied from 1000 to 4000 feet per second, while mass and projectile diameter were held constant. Three of the control specimens had mechanically drilled holes, while the other three were undamaged. Following visual and x-ray inspection (using radio-opaque dye to improve contrast) these specimens were tested to destruction while under tension in a universal testing machine, to determine their ultimate strengths.

III. SPECIMENS

A. MANUFACTURE OF PLATES

All plates used in the test program were constructed from 12-inch wide rolls of UCC Thornel 300 (untwisted) Graphite Fibers, in a Rigidite 5208 matrix manufactured as a B-stage prepreg by the NARMCO Materials Division of the Celanese Corporation. Sixteen-inch square plates were manufactured in the Naval Postgraduate School Composite Laboratory. The procedures set forth by the material manufacturer and Linnander [Ref. 1] were followed. These procedures yielded a 65% fiber content by volume [Ref. 2]. The laminate orientation code for this eight lamina lay-up [Ref. 3] was $(0/\pm 45°/0)_s$ as indicated in Fig. 1. After the proper cure, the panels were sectioned as necessary with a diamond cut-off wheel. The diamond cut-off wheel produced an extremely smooth edge without any apparent edge damage or delamination of the specimens.

B. PREPARATION FOR BALLISTIC RANGE

The plates were cut in five-inch widths to be compatible with the ballistic range test-bed. The test-bed (shown in Fig. 2) allowed a five-inch wide specimen to be clamped on it and exposed a four-by-four inch area for ballistic impact.

C. PREPARATION FOR RESIDUAL STRENGTH TESTS

After a five-inch wide specimen was ballistically impacted, it was removed and further reduced in width to 1.5 inches by

cutting off the edges with the diamond wheel. As the width was reduced, the position of the ballistic hole was kept as close as possible to the center. Two 2 x 1.5 inch fiberglass/epoxy end tabs were sanwiched on each end of the specimens. The edge of the tab closest to the ballistic damage area was tapered to a 15° angle prior to installation. Because of the tapering of the tab, the loading applied by the tensile testing machine was transmitted gradually and uniformly into the specimen. The tabs were attached using APCO 210 low viscosity epoxy resin with APCO 180 catalyst.

IV. TEST APPARATUS AND PROCEDURES

A. BALLISTIC RANGE

All damage inflicted on the test specimens was done at the Naval Postgraduate School Ballistic Range. The ballistic facility was developed with the idea of being able to make custom-made loads based on the reloading data that were gathered through previous testing and retesting. These data provided valuable information on ballistics that enabled testing to be conducted as desired. A 22-caliber barrel was used because it simulated a shell fragment from a near-by antiaircraft burst, and because it allowed a great degree of flexibility in testing. Figure 3 illustrates this barrel as it is set up in the return-to-battery-machine rest. For a detailed description of the range facility, see Davis [Ref. 4].

Before any test loads were made at the ballistic range a careful study of the results by Davis [Ref. 4] was completed. These results included six "Velocity vs. Powder Weight" graphs for the 22-caliber bullet. The graph that plotted the results for the 45 grain bullet with the IMR 3031 powder contained the majority of the test velocity spectrum desired. The IMR 3031 powder gives a nearly linear velocity increase with changes in powder weight from 2650 feet per second to 4000 feet per second; however the velocity spectrum desired was 1000 feet per second to 4000 feet per second. The velocities from 1000 feet per second to 2650 feet per second had to be obtained without the aid of previously tested data.

Attempts to achieve velocities below 2650 feet per second with IMR 3031 powder initially proved to be inconsistent. It was concluded that the small amount of powder in the large case caused incomplete burning in most cases. By inserting one-half grain of dacron filler and lightly tamping it in the case after the powder charge was loaded, consistent results were obtained from 1400 feet per second to 2650 feet per second with the IMR 3031 powder. To reach the 1000 feet per second velocity, a pistol powder, UNIQUE, was found to be effective. UNIQUE is a fast burning powder that gives a short duration pressure build-up behind the bullet; hence a lower velocity. As when using a light charge of IMR 3031 powder, a one-half grain of dacron filler was necessary to give consistent results with UNIQUE.

Previously tested data were available when changing the mass of the projectile. The 27.5 grain projectile was loaded with IMR 3031 powder while the 63 grain bullet used IMR 4320 powder. Other powders and results were available to use but the IMR 4320 powder, like the IMR 3031 powder, gives nearly linear velocity changes with powder weight changes. With a nearly linear velocity vs. powder weight curve, small modifications in powder weight could be made with predictable results.

Once a desired velocity and mass combination was reached, two additional practice shots were fired to confirm the desired velocity. In some cases, slight modifications to the powder weight had to be made. Again, two additional

shots were fired to confirm the new velocity. By using this iterative method, the specimens were able to be impacted at the desired location and with the desired velocity.

B. INSPECTION

1. Visual Examination

The plates were examined visually and damage measured using a dial caliper on both entrance and exit sides. See Appendix A for results.

2. Microscopic Examination

During the first test series the damaged specimens were cut transversely through the center of the hole, and a section along this line was removed for examination. These samples were mounted in cold-set plastic and polished for microscopic examination. Figure 4 shows a specimen ready for the microscope. The samples were examined and photographed at a magnification of 80X. Typical results are shown in Figures 5 through 11.

3. Ultrasonic Inspection

Specimens in the first test series were inspected ultrasonically using an Automation Industries, Inc., Sperry Division, Model UM-771 Reflectoscope Ultrasonic Testing Machine. The machine was equipped with 2.25 MHz and 5.0 MHz zero degree transducers. Also 2.25 MHz transducers with sound input angles of 45, 60 and 90 degrees were available. All possible combinations of transducers were tried. The difference between the damaged and the non-damaged area could not be detected via ultrasonic testing.

Direct liaison was conducted with a well-known firm that deals in ultrasonic testing. This firm felt that the frequency range of the available equipment was too high. A frequency of 1 MHz or lower yielded excellent results on their equipment. Because of the available equipment, in-house ultrasonic testing was terminated.

4. X-ray Inspection

Two types of x-ray machines were used. For the first series of tests a General Electric LX-40 Portable Industrial X-Ray Unit was used. The minimum intensity and duration setting of this device is 70 kilovolts and 10 seconds. At this setting the x-ray photographic plate was so washed out that it was difficult to detect the specimen, let alone any damage to it. Use of this machine was terminated after the first test series.

For the second test series a more sophisticated x-ray machine, a Phillips Model Super M-80, was used. This has a much lower intensity capability (45 vice 70 kilovolts) and has an automatic duration control. In the automatic mode the duration of the x-ray exposure is controlled by an exposure sensing device in the vicinity of the photographic plate; for the specimens used in these tests the automatically selected duration was 11 milliseconds, as compared with the 10-second minimum exposure of the industrial machine! Results of these inspections were usable, but only with difficulty. Contrast was weak, but it was possible to make out the outline of the damaged area. Next, a radio-opaque

dye (a 29% solution of iodine in meglumine diatrizoate and sodium diatrizoate), was injected into the damaged area. This solution greatly increased the x-ray absorption where present, and thus improved the contrast dramatically. The resulting x-ray photographs are easily readable, even by the untrained observer. Figures 12, 13, and 14 compare both x-ray and light photographs of the same specimens, while Figures 15 through 19 show x-ray photographs of the specimens used in the final test sequence. Note that the x-ray photographs show a dark ring of delamination around the hole as well as splitting and delamination in the 0° direction. This delaminated ring was confirmed by sectioning and microscopic examination.

C. TENSILE TESTS

The tensile testing done in the third test sequence was conducted in a 300,000 pound RIEHLE test machine set at a 15,000 pound maximum scale. The specimen width corresponded to the width of the machine's jaws, which helped in specimen alignment. Once the specimens were aligned, the machine was started and loading commenced at a rate of .025 inches/minute. As the loading continued, the fibers above and below the hole that were previously delaminated due to ballistic damage began to separate further outward from the specimen. There was no apparent delamination of the other fibers at this point but the previously damaged outer fibers protruded from the specimen further as the load increased. The loading continued and the fibers protruded further until the specimen broke.

The maximum loading at failure was recorded. Figures 20, 21, and 22 illustrate the sequence of events leading to and including failure of a specimen. The outer laminae of the composite specimens (0° direction) were the only laminae that experienced this separation and protruding. The second ply (45° direction) appeared to remain intact until final failure. The three mechanically drilled control specimens also experienced this separating and protruding above and below the hole, even though they did not have any prior delamination caused by ballistic damage. As loading was applied to these specimens they reacted the same way as the ballistically damaged specimens behaved up to and including failure. The undamaged control specimens showed no sign of physical change while being loaded until they broke.

In the specimens tested that contained holes, which included damaged and drilled holes, the fracture line was at the hole or within the influence area of the hole. By passing a +45° line and a -45° line through the center of the hole and noting where these lines intersected the edge of the specimens, the influence area of the hole could be described. All the lines of failure passed within this 1.5 inch-by-1.5 inch area.

V. DISCUSSION OF RESULTS

On the basis of the experimental work undertaken in this program some general observations concerning the behavior of laminated composite plates subjected to ballistic impact can be made.

When a graphite-epoxy plate is subjected to ballistic damage, the resulting hole is round but not smooth, and the material at the edge of the hole is delaminated. Fibers in the outer lamina on the exit side, which were broken by the passage of the projectile, tend to delaminate and separate, and this damage extends for some distance from the hole in the fiber direction. Fibers which are not broken by the projectile, on the other hand, do not delaminate, except perhaps in the immediate vicinity of the hole. In addition, only fibers from the outermost lamina delaminate and separate; fibers from the 45° laminae, although broken, did not delaminate, except in the immediate vicinity of the hole. Thus the damaged area is roughly elliptical in shape, with the major axis in the direction of the fibers of the outer exit-side lamina. Figures 23 and 24 show the variation of damage area with projectile velocity. As can be seen, the damage area decreases as velocity is increased. In addition, at low velocity the separation of the fibers was very pronounced. As the velocity of the projectile increased up to the maximum tested velocity of 4000 feet per second, the separation of the fibers became less but was still visible.

The effect of mass variation did not appear to be a major factor in damage area or extent of fiber separation due to ballistic impact. The damage done to the specimens was nearly uniform for the three masses investigated. Figures 12, 13, and 14 depict the variable-mass specimens and the damage experienced.

In the third sequence of tests, in addition to evaluating the visual and x-ray damage inspection procedures, a comparison was made between the residual strengths of ballistically damaged specimens and the residual strength of the control specimens. To compute the average stress at failure it was necessary to know the cross-sectional area remaining after ballistic damage. The net width was measured on the specimen, with the width of the damaged area being determined either visually or by x-ray means. The thickness was assumed to be 0.040 inches, based on an average lamina thickness of 0.005 inches. Small variations in the thickness of laminates result primarily from changes in matrix thickness; fiber content remains constant. Thus, it is the thickness of the low strength, low modulus component which changes, and the strength and stiffness of the composite, and the stresses in the fibers, are not appreciably altered. Therefore, for comparisons between laminates of the same lay-ups experiencing the same loading it is common practice to use a nominal thickness based on an average lamina thickness.

Figure 25 shows the variation of the residual strength with visible damage area. This plot shows that the ultimate

average stress ("residual strength") across the material remaining after damage is nearly constant, i.e., is independent of the ballistic damage area. The residual strength level shown agrees within 1% with the residual strength exhibited by the drilled-hole control specimens. The loss in strength produced by the hole averages 5%; this result compares favorably with previous work [Refs. 5, 6] which indicated a loss of strength of about 10% for ballistic damage. It should be emphasized that "strength" or "residual strength" used in this context refers to the ultimate average stress rather than to the remaining load-carrying capability of the specimen. The latter quantity depends upon the amount of material remaining, i.e., upon the width of the specimen less the width of the damage area; the smaller the damage width, the greater the load-carrying capability remaining. However, regardless of the size of the damaged area, or of the damage width, the average stress at failure for the ballistically damaged specimens was essentially constant.

Figure 26 shows the variation of residual strength with x-ray detected damage area. Again the ultimate average stress is essentially constant, but in this case the residual strength is greater than that of the undamaged control specimens. Obviously, this finding cannot be correct: the explanation is that fibers which have been delaminated but not broken around the hole are included in the damaged area shown on the x-ray picture. These fibers actually do carry load,

but are considered to be removed when calculating residual strength based on x-ray information. The x-ray data, then, result in an overestimation of residual strength.

Figure 27 plots residual strength vs. projectile velocity and shows that the residual strength is essentially independent of the velocity of the impacting projectile. Figure 28 shows the variation in visible damage width as a function of projectile velocity, while Figure 29 shows the variation in visible damage length as a function of projectile velocity. Consideration of these figures leads to the conclusion that for the specimens tested and the loading scheme (i.e., uniaxial tension) used in this test series, damage length has little or no effect on residual strength. Since projectile diameter was not varied, and velocity changes had little effect on damage width, the effect of damage width on residual strength was not determined. Changes in projectile velocity did cause changes in damage length, but as can be inferred from Figure 27, these changes in damage length did not result in changes in residual strength.

This does not mean, however, that there is no need to know the extent of damage in the tensile direction, and the extent of delamination around the hole. Even though the results of the static tests conducted were not affected noticeably by these damage parameters, in actual use other types of loadings, including compression and shear loads, occurring in varying cycles and intensities, can be expected. The damage around the hole can be expected to nucleate further

damage under these fatigue loading conditions, unless properly repaired. Thus it is of interest to know the extent of the damage experienced, even if it does not affect the static strength of the specimen greatly. The x-ray inspection technique used in this program is a way to determine the extent of the damage around a hole, including the delamination which is not visible at the surface.

VI. CONCLUSIONS

A. The velocity of the impacting projectile has a major effect on the size of the damaged area produced by a ballistic impact on a thin, flat, laminated composite panel. Lower projectile velocities produce much more separation of fibers and delamination at the exit surface than do higher velocities.

B. The velocity of the impacting projectile has little effect on the residual strength in tension of the damaged graphite-epoxy plates.

C. There is little or no difference between a drilled hole and a ballistically-produced damage area of equal "across-load" diameter when comparing residual strengths.

D. Projectile mass variations (with projectile velocity and diameter held constant) had no apparent effect on the size of the damaged area.

E. X-ray inspection can provide a relatively easy and accurate method for evaluating the extent of internal damage in a composite plate, provided a hole exists which will permit the introduction of a radio-opaque dye such as was used here. If no hole exists, detection of internal damage by means of x-ray examination is more difficult.

VII. RECOMMENDATIONS

A. The fiber directions of the two outermost plies on each side of a laminated composite panel should be different, so as to control delamination and separation of fibers and thus localize damage in the event of ballistic impact on the panel.

B. X-ray inspection techniques utilizing radio-opaque dyes to enhance contrast in areas of damage should be investigated further.

LAMINA FIBER ORIENTATION

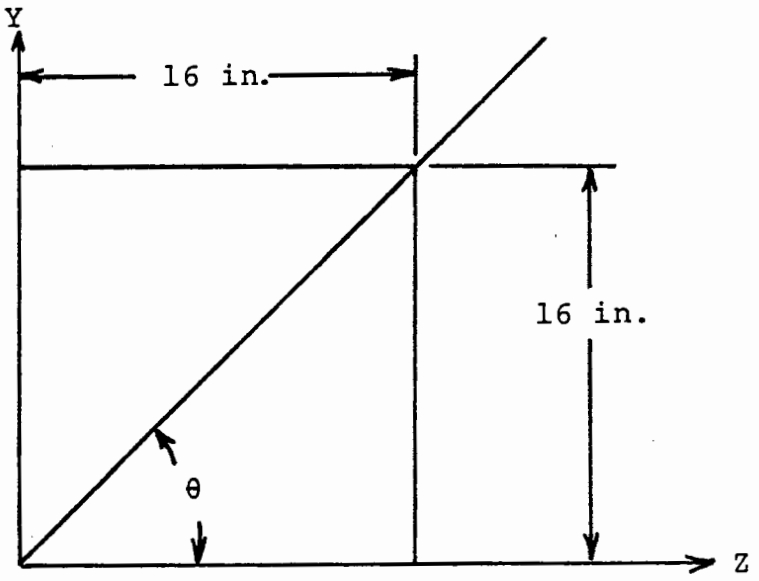

	LAMINA	θ
.040 in.	1	0
	2	+45
	3	-45
	4	0
.005 in.	5	0
	6	-45
	7	+45
	8	0

Figure 1 - ORIENTATION OF LAMINA ON TEST LAMINATED PLATE.

Figure 2

BALLISTIC RANGE TEST-BED FOR GRAPHITE-EPOXY SPECIMENS

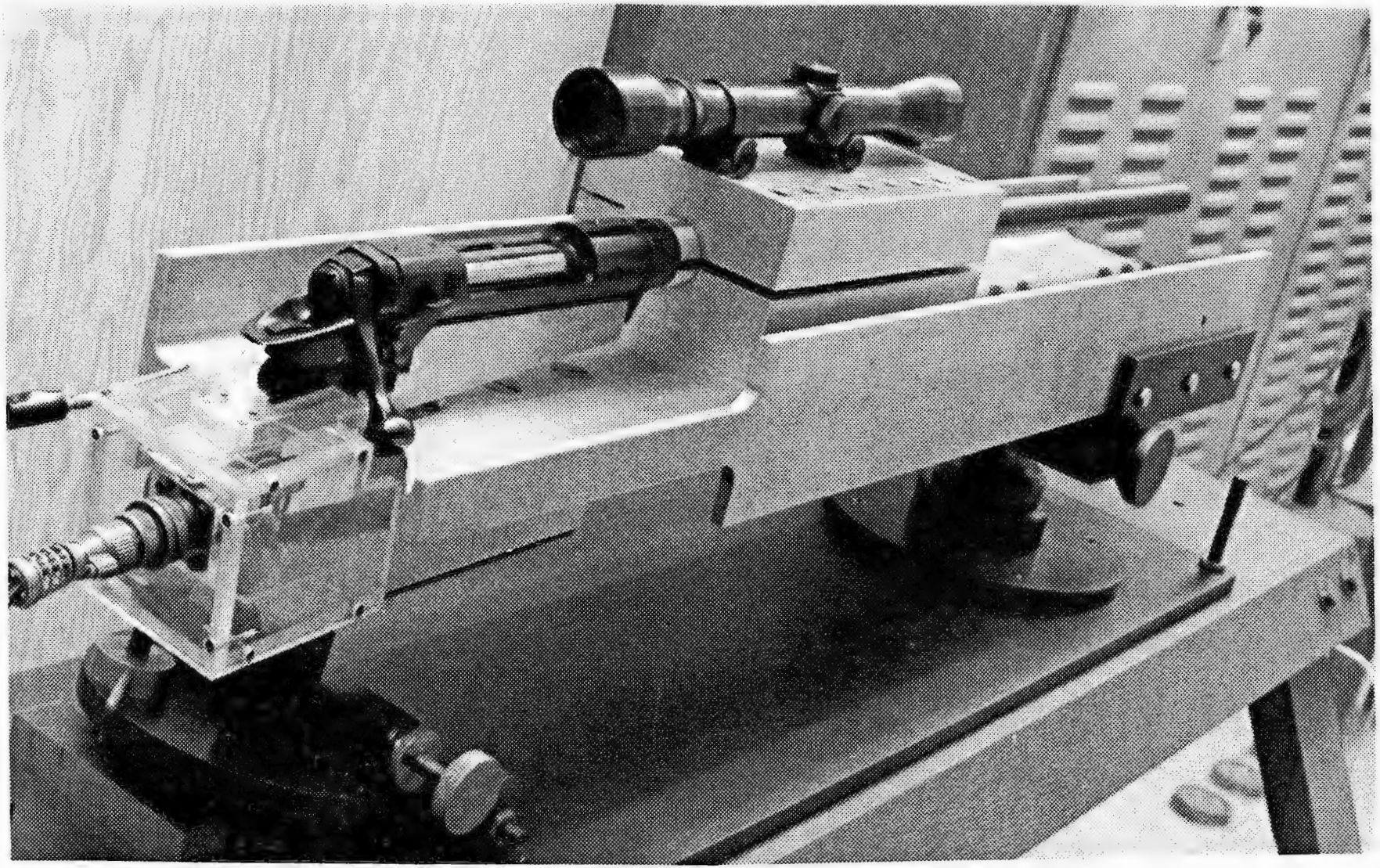

Figure 3 - RETURN-TO-BATTERY MACHINE REST

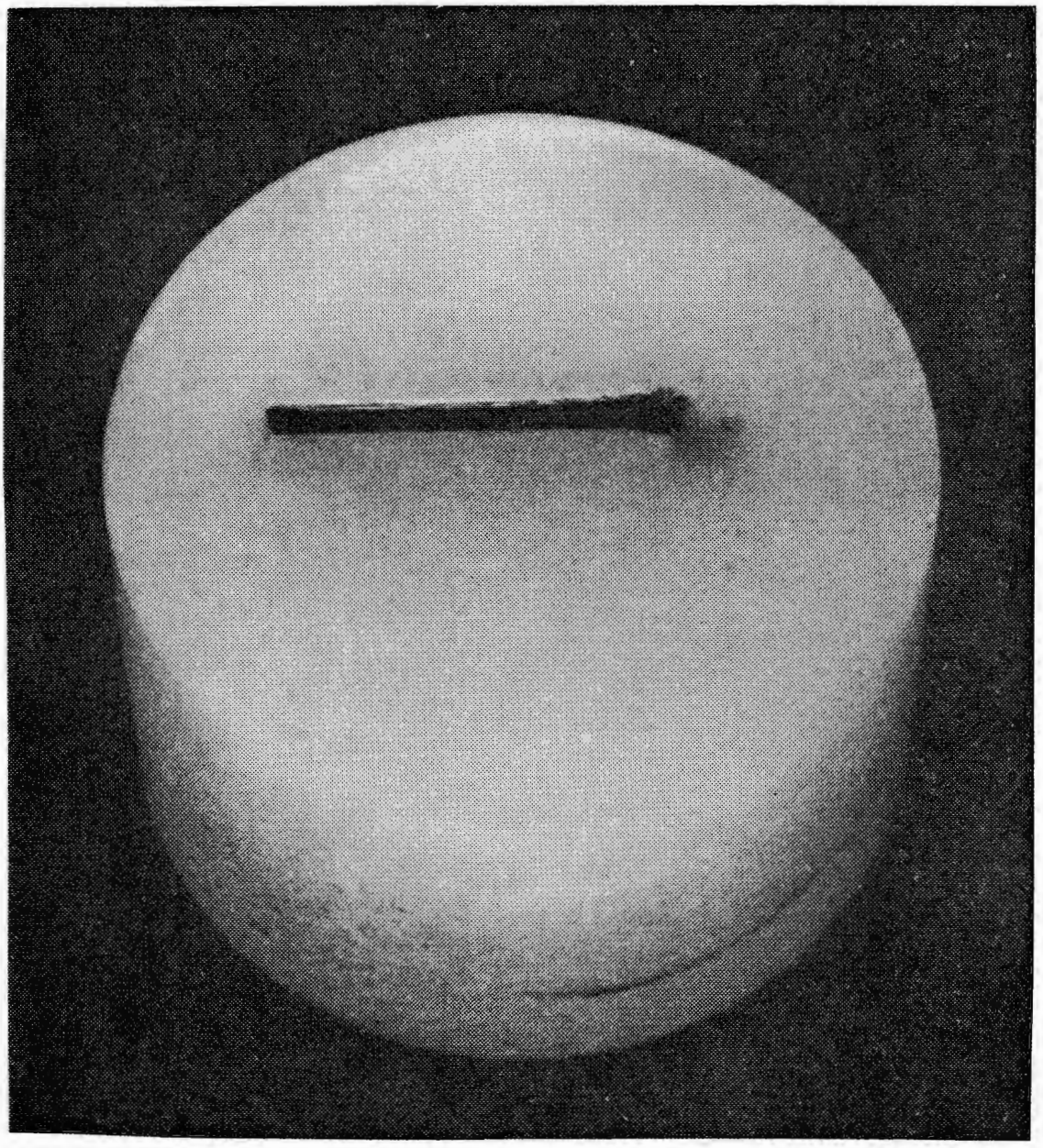

Figure 4 - A SPECIMEN READY FOR THE MICROSCOPE

ENTRY SIDE

EXIT SIDE

ENTRY SIDE

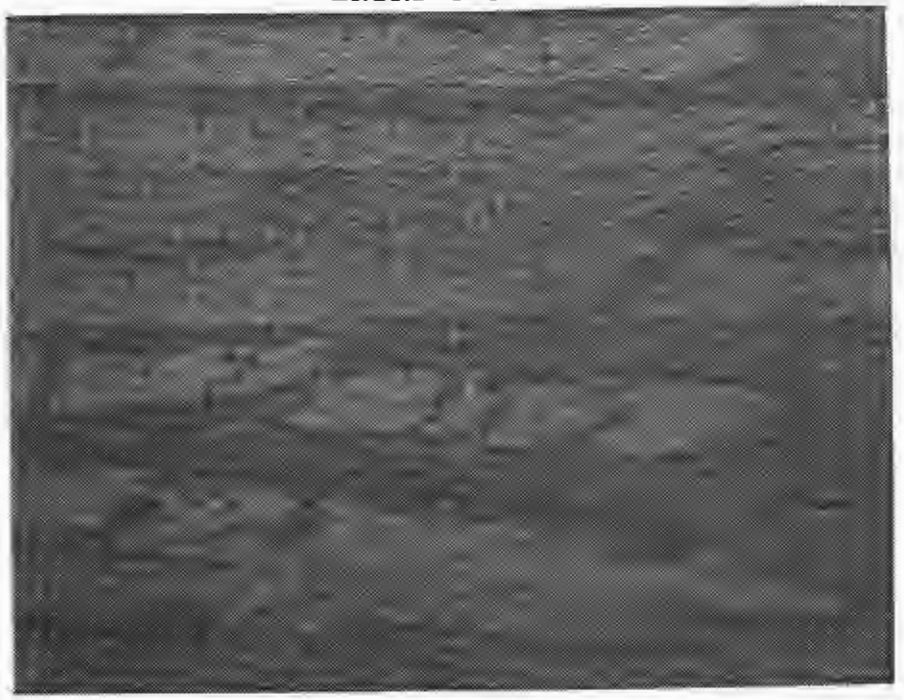

EXIT SIDE

Figure 5 - MICROGRAPH OF SPECIMEN DAMAGED AT 1014 FPS

ENTRY SIDE EXIT SIDE

ENTRY SIDE

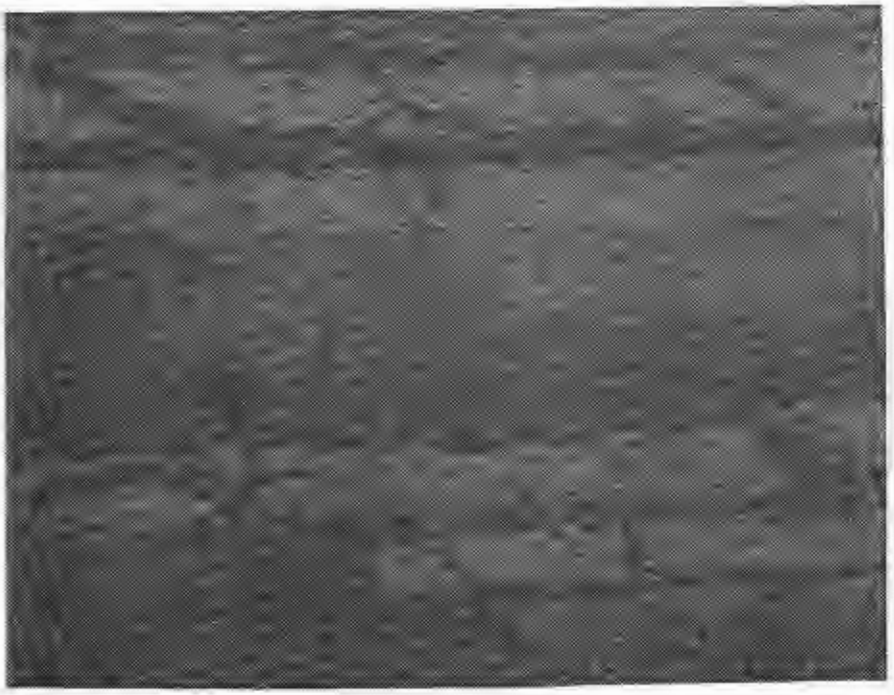

EXIT SIDE

Figure 6 - MICROGRAPH OF SPECIMEN DAMAGED AT 1410 FPS

ENTRY SIDE

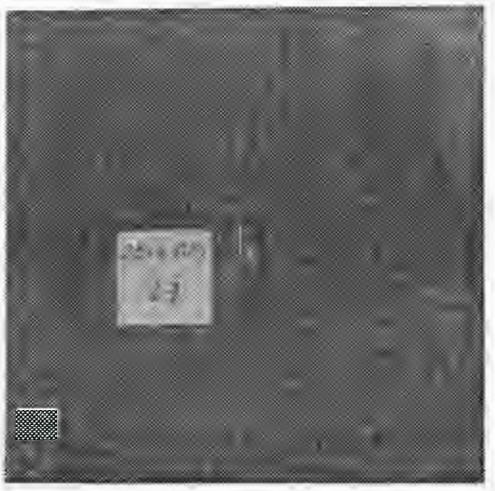

EXIT SIDE

ENTRY SIDE

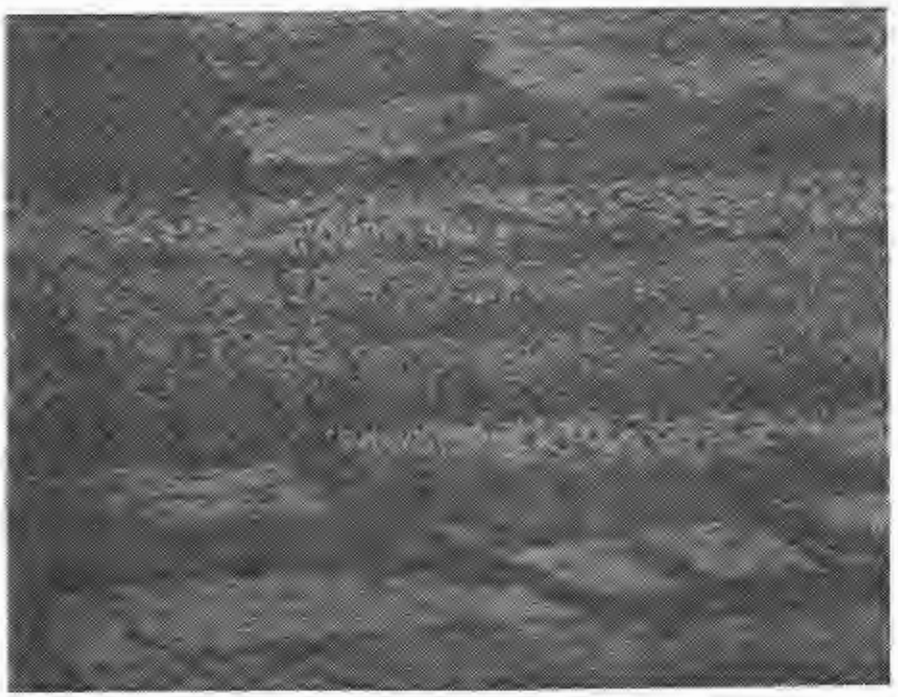

EXIT SIDE

Figure 7 - MICROGRAPH OF SPECIMEN DAMAGED AT 2019 FPS

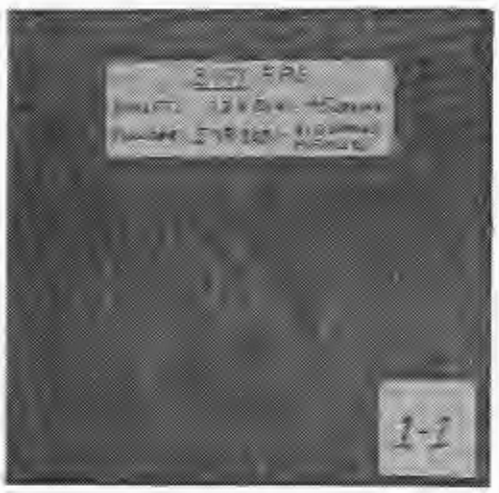

ENTRY SIDE

EXIT SIDE

ENTRY SIDE

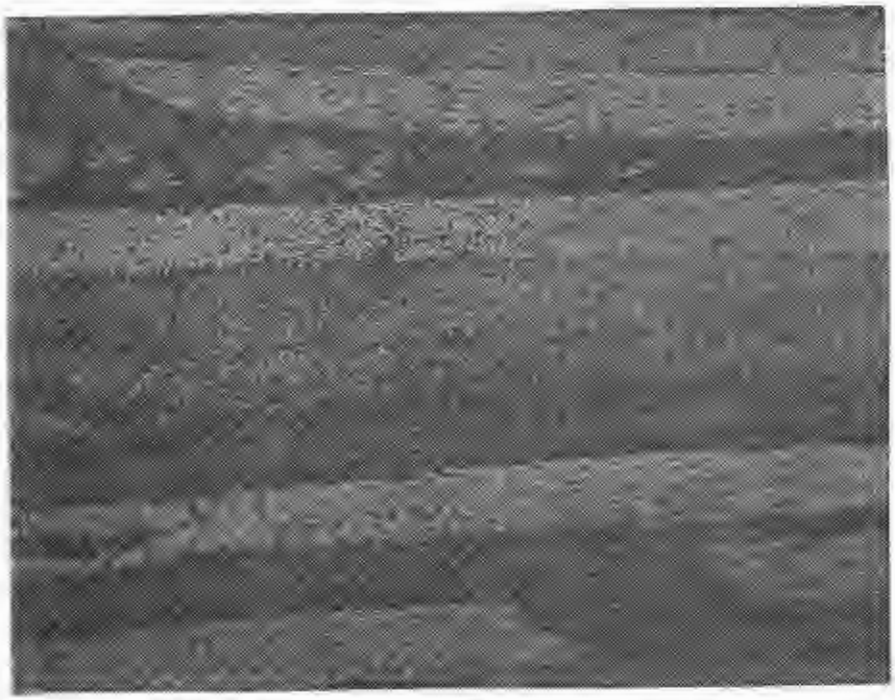

EXIT SIDE

Figure 8 - MICROGRAPH OF SPECIMEN DAMAGED AT 2471 FPS

ENTRY SIDE EXIT SIDE

ENTRY SIDE

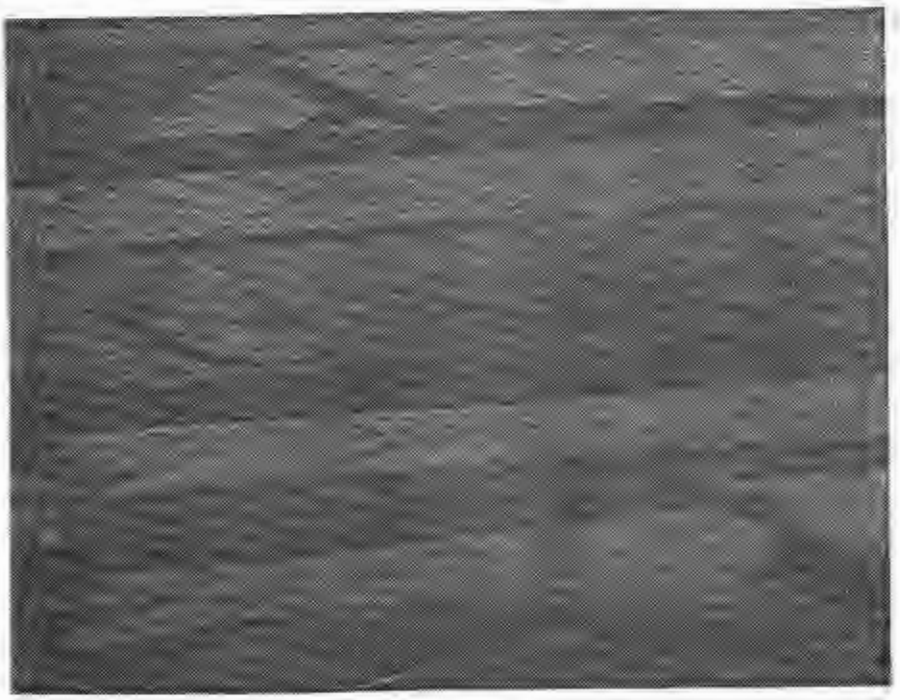

EXIT SIDE

Figure 9 - MICROGRAPH OF SPECIMEN DAMAGED AT 3123 FPS

ENTRY SIDE EXIT SIDE

ENTRY SIDE

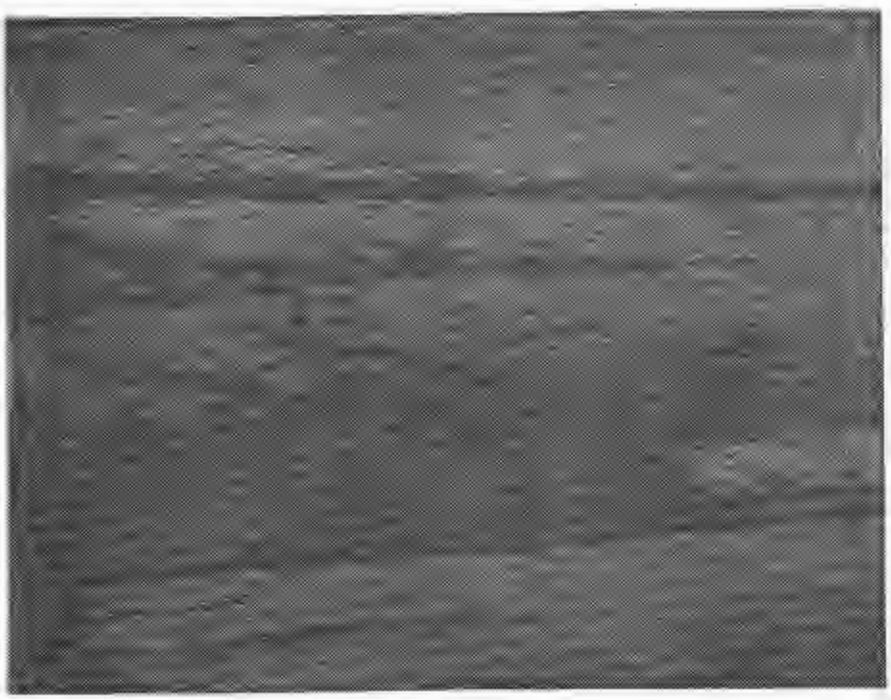

EXIT SIDE

Figure 10 - MICROGRAPH OF SPECIMEN DAMAGED AT 3487 FPS

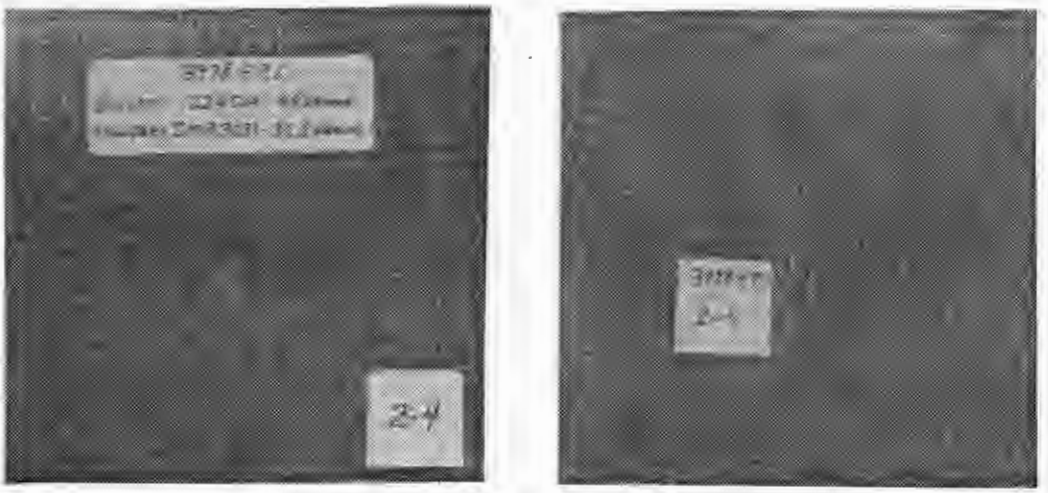

ENTRY SIDE EXIT SIDE

ENTRY SIDE

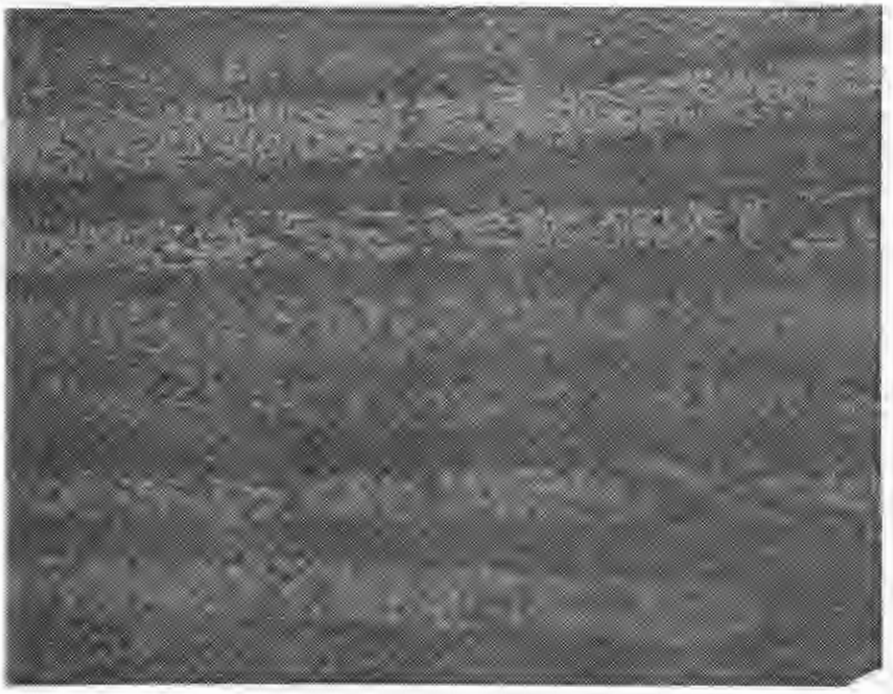

EXIT SIDE

Figure 11 - MICROGRAPH OF SPECIMEN DAMAGED AT 3978 FPS

ENTRY SIDE EXIT SIDE

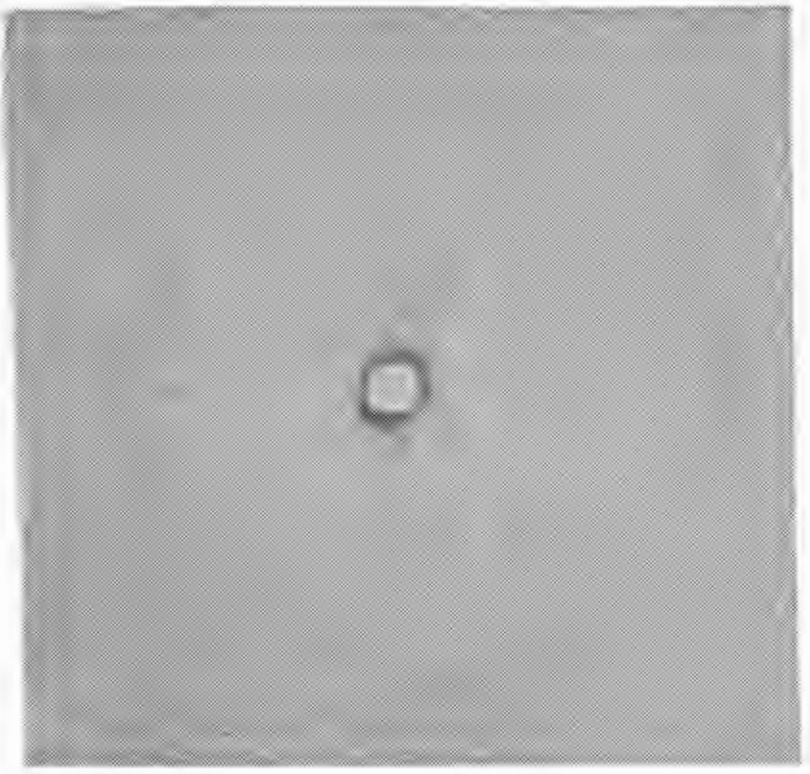

X-RAY (DYE USED)

Figure 12 - COMPARISON OF X-RAY AND PHOTOGRAPH OF SPECIMEN DAMAGED AT 3407 FPS

ENTRY SIDE EXIT SIDE

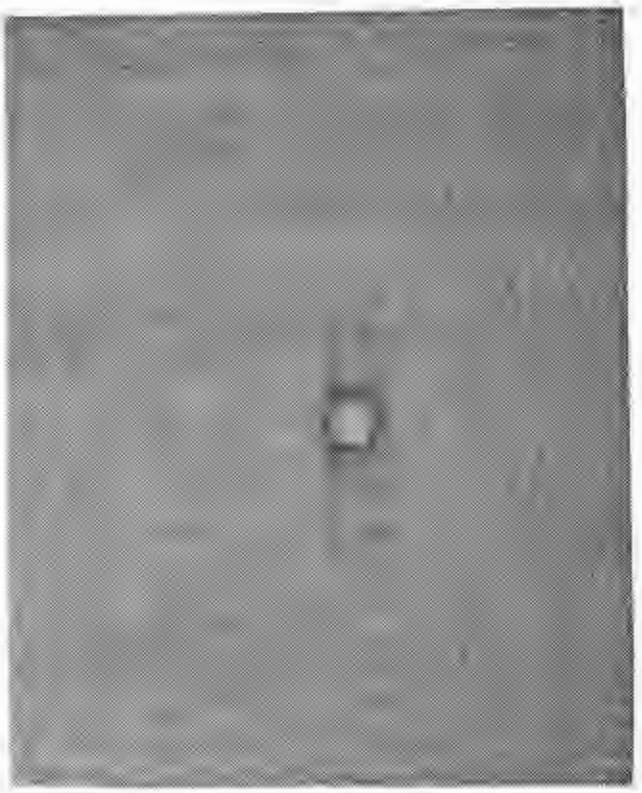

X-RAY (DYE USED)

Figure 13 - COMPARISON OF X-RAY AND PHOTOGRAPH OF SPECIMEN DAMAGED AT 3296 FPS

ENTRY SIDE

EXIT SIDE

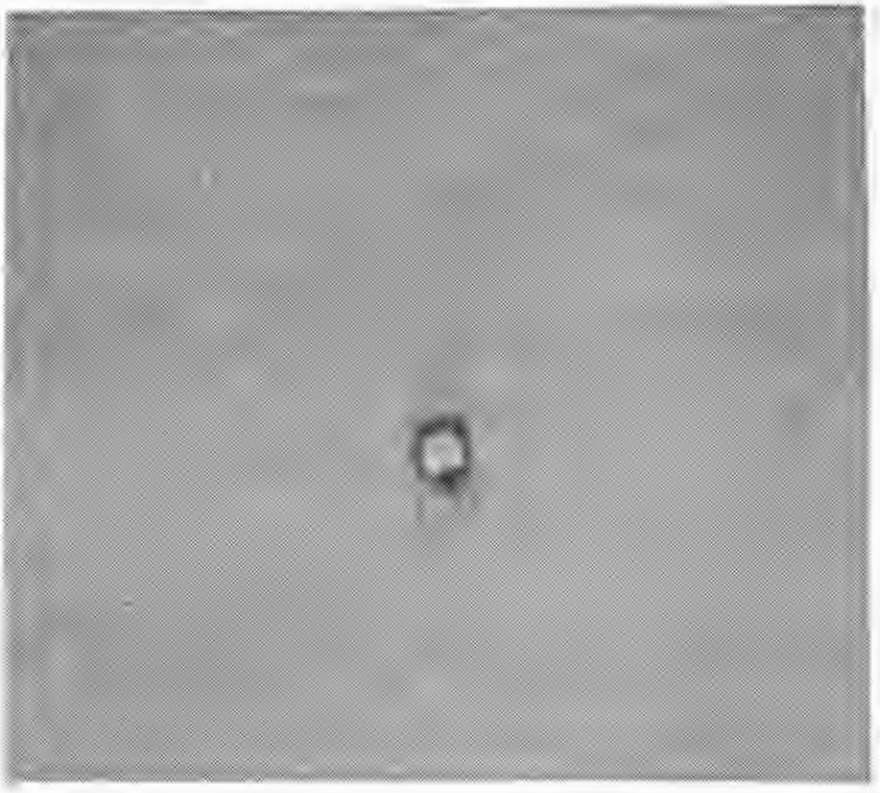

X-RAY (DYE USED)

Figure 14 - COMPARISON OF X-RAY AND PHOTOGRAPH OF SPECIMEN DAMAGED AT 3348 FPS

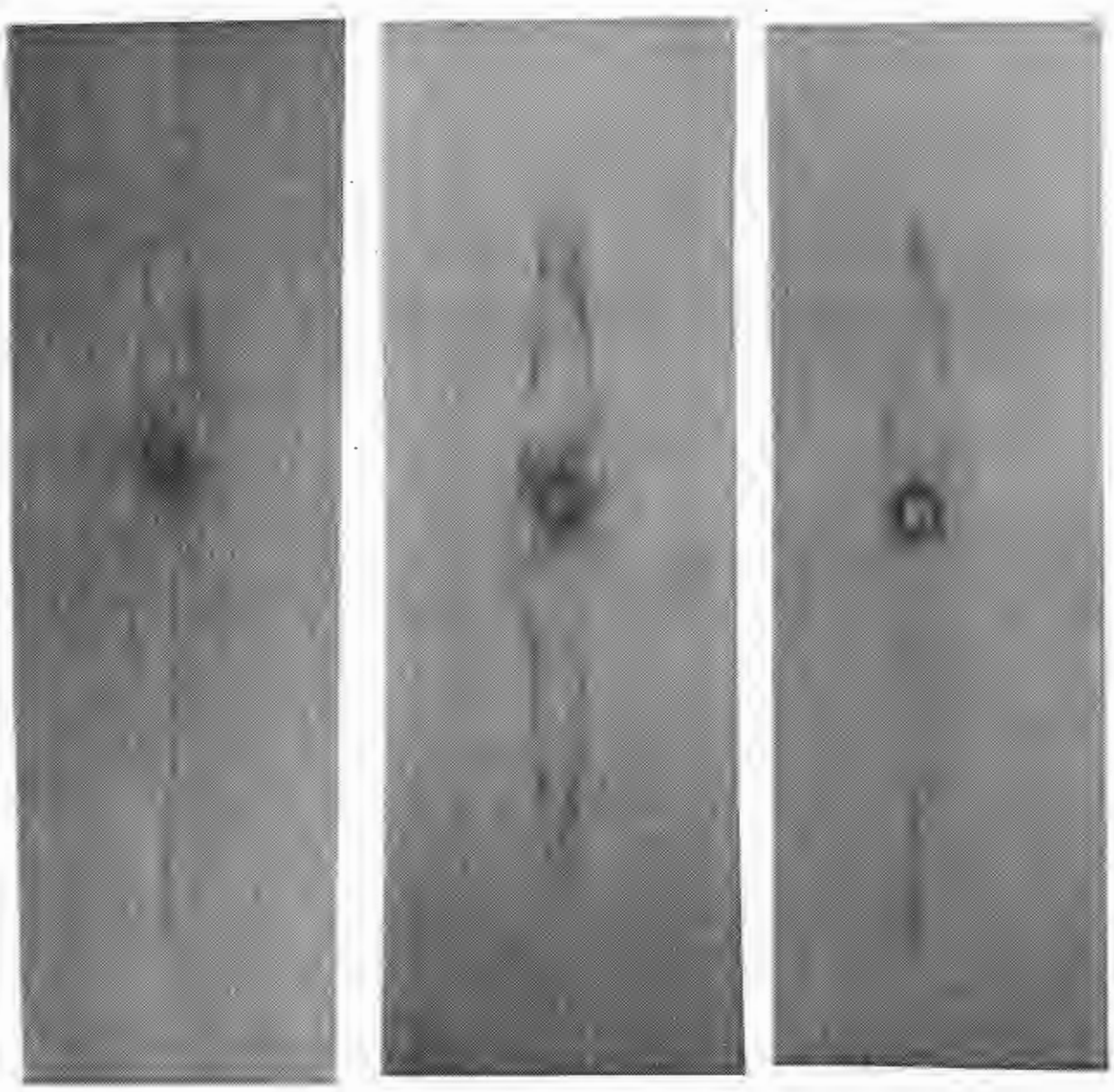

A. DAMAGE AT 980 FPS B. DAMAGE AT 993 FPS C. DAMAGE AT 1046 FPS

Figure 15 - X-RAYS (WITH RADIO-OPAQUE DYE) OF DAMAGED SPECIMENS

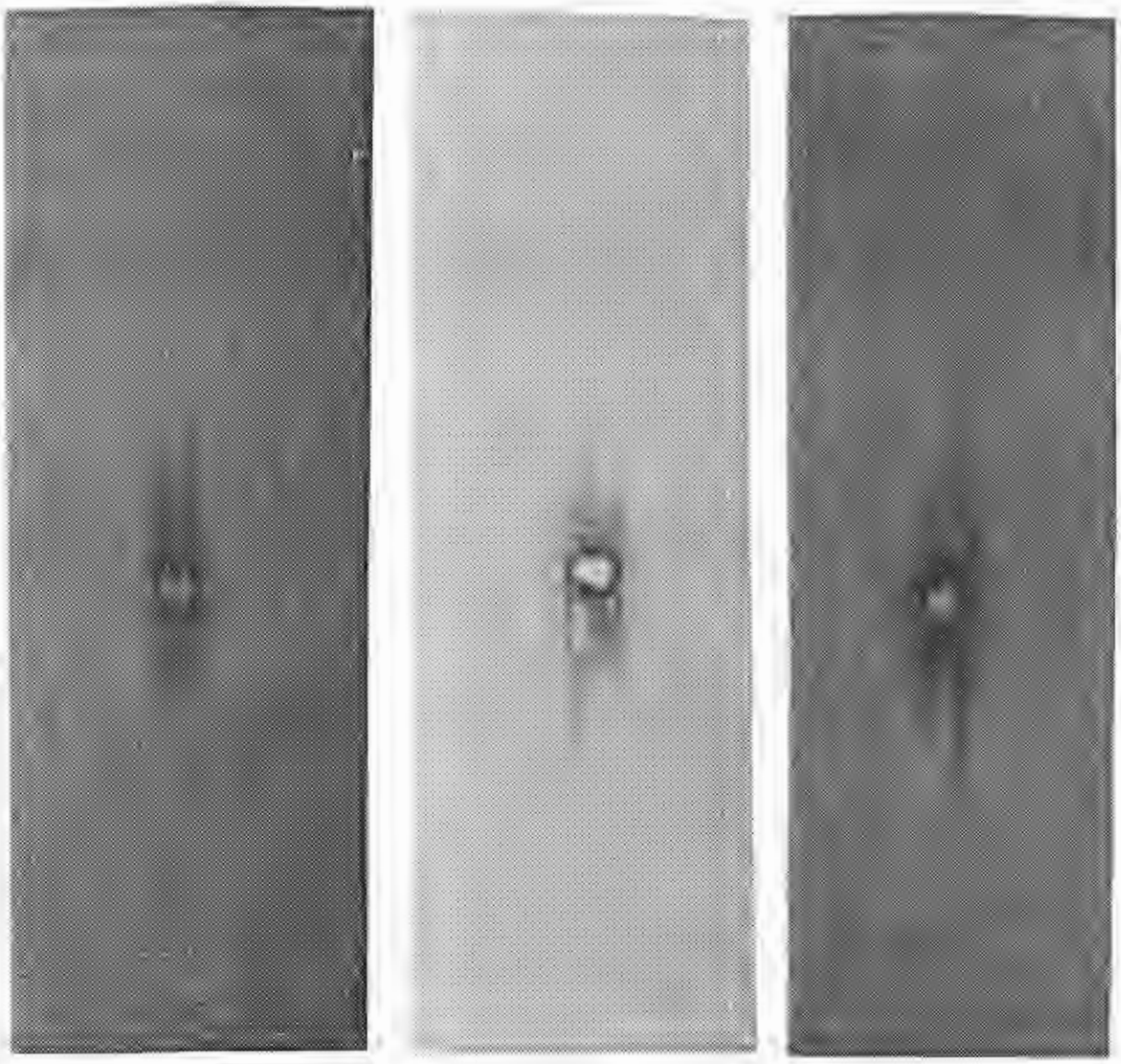

A. DAMAGE AT 2033 FPS B. DAMAGE AT 2058 FPS C. DAMAGE AT 2031 FPS

Figure 16 - X-RAYS (WITH RADIO-OPAQUE DYE) OF DAMAGED SPECIMENS

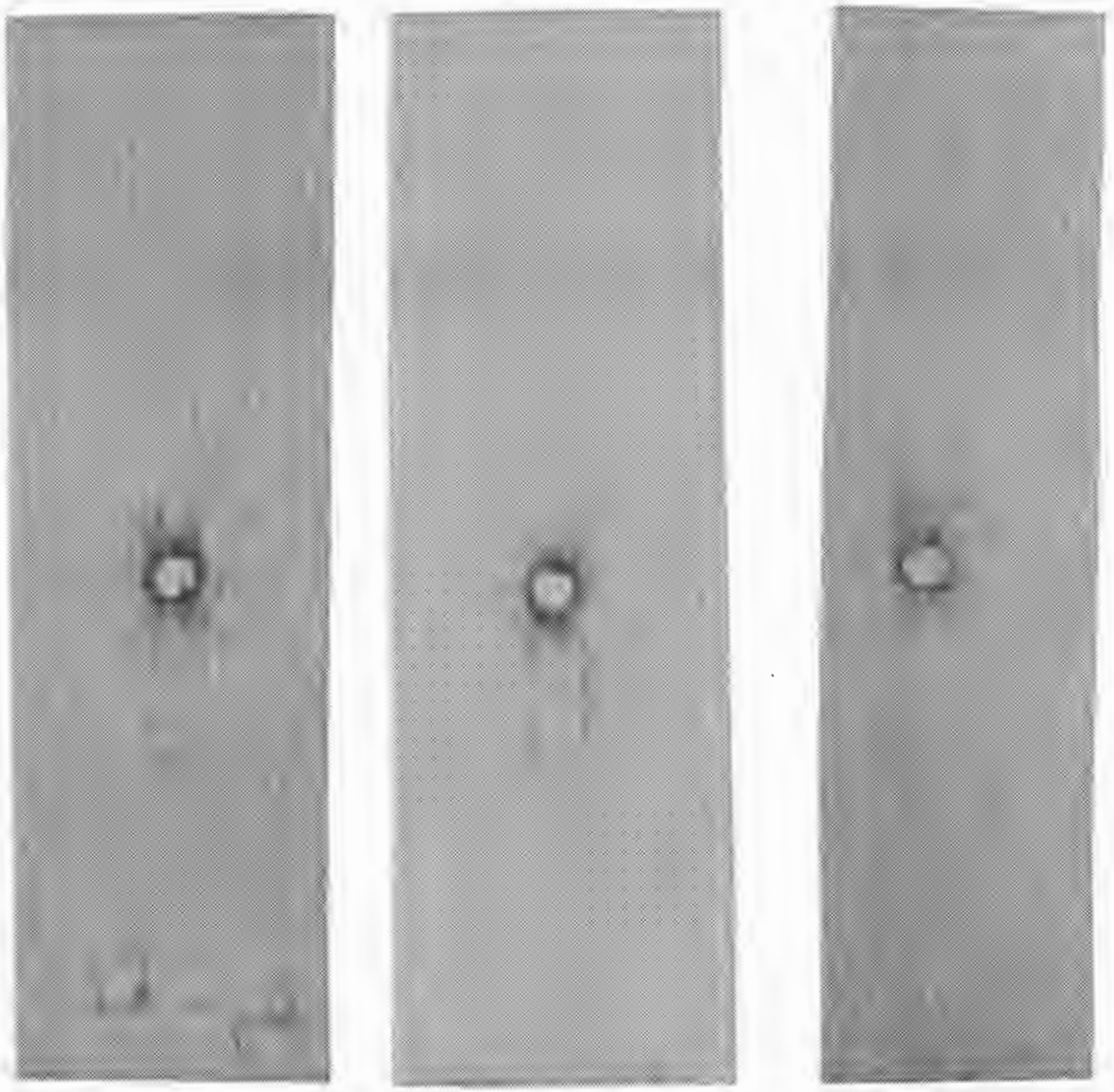

A. DAMAGE AT 2982 FPS B. DAMAGE AT 3026 FPS C. DAMAGE AT 3098 FPS

Figure 17 - X-RAYS (WITH RADIO-OPAQUE DYE) OF DAMAGED SPECIMENS

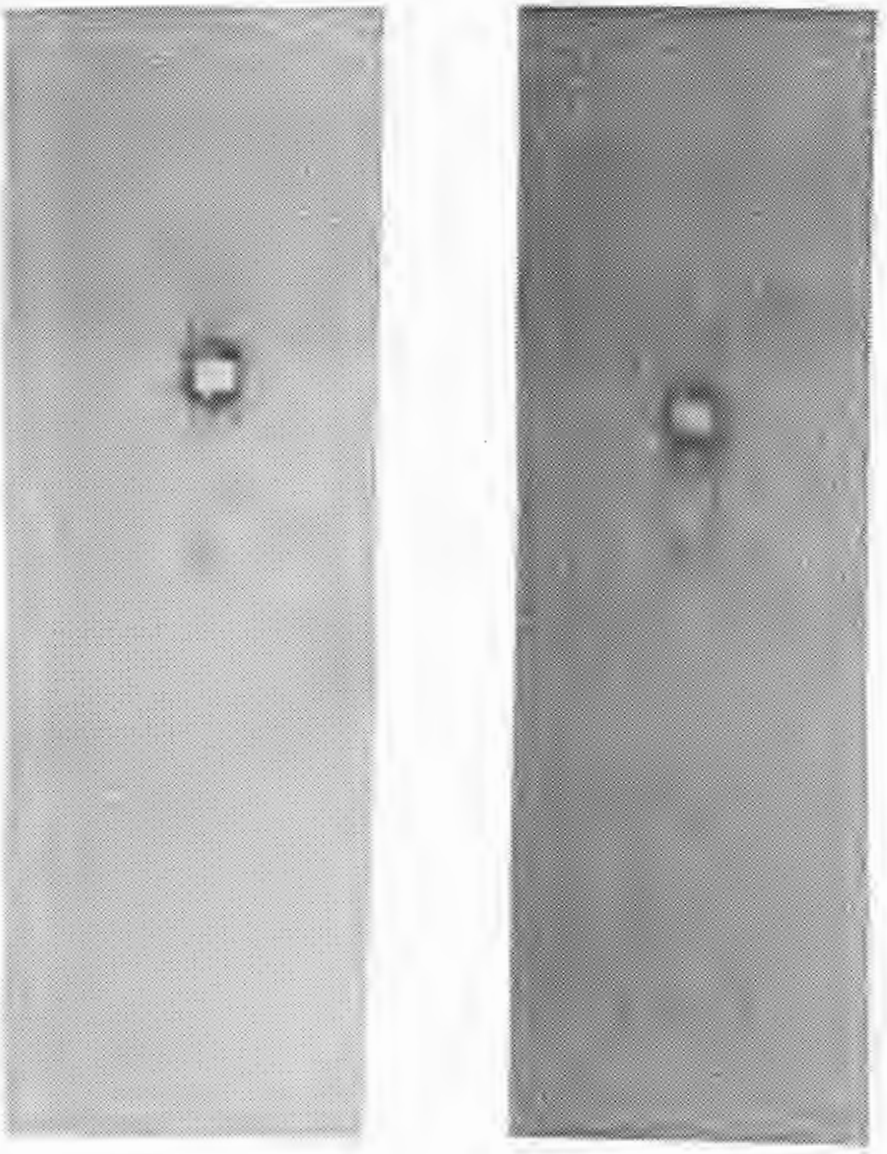

A. DAMAGE AT 3534 FPS B. DAMAGE AT 3517 FPS

Figure 18 - X-RAYS (WITH RADIO-OPAQUE DYE) OF DAMAGED SPECIMENS

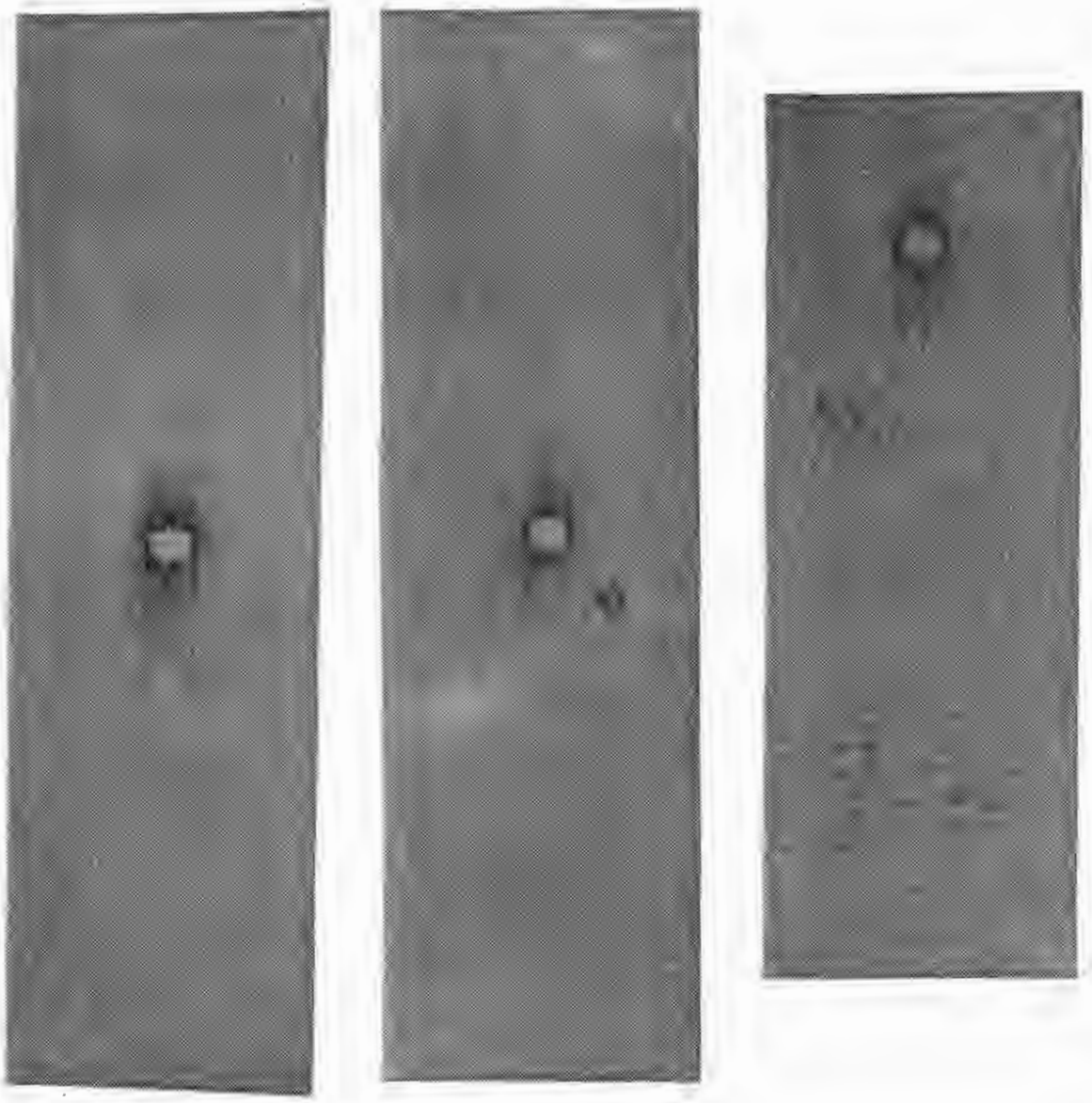

A. DAMAGE AT 4029 FPS B. DAMAGE AT 3994 FPS C. DAMAGE AT 4058 FPS

Figure 19 - X-RAYS (WITH RADIO-OPAQUE DYE) OF DAMAGED SPECIMENS

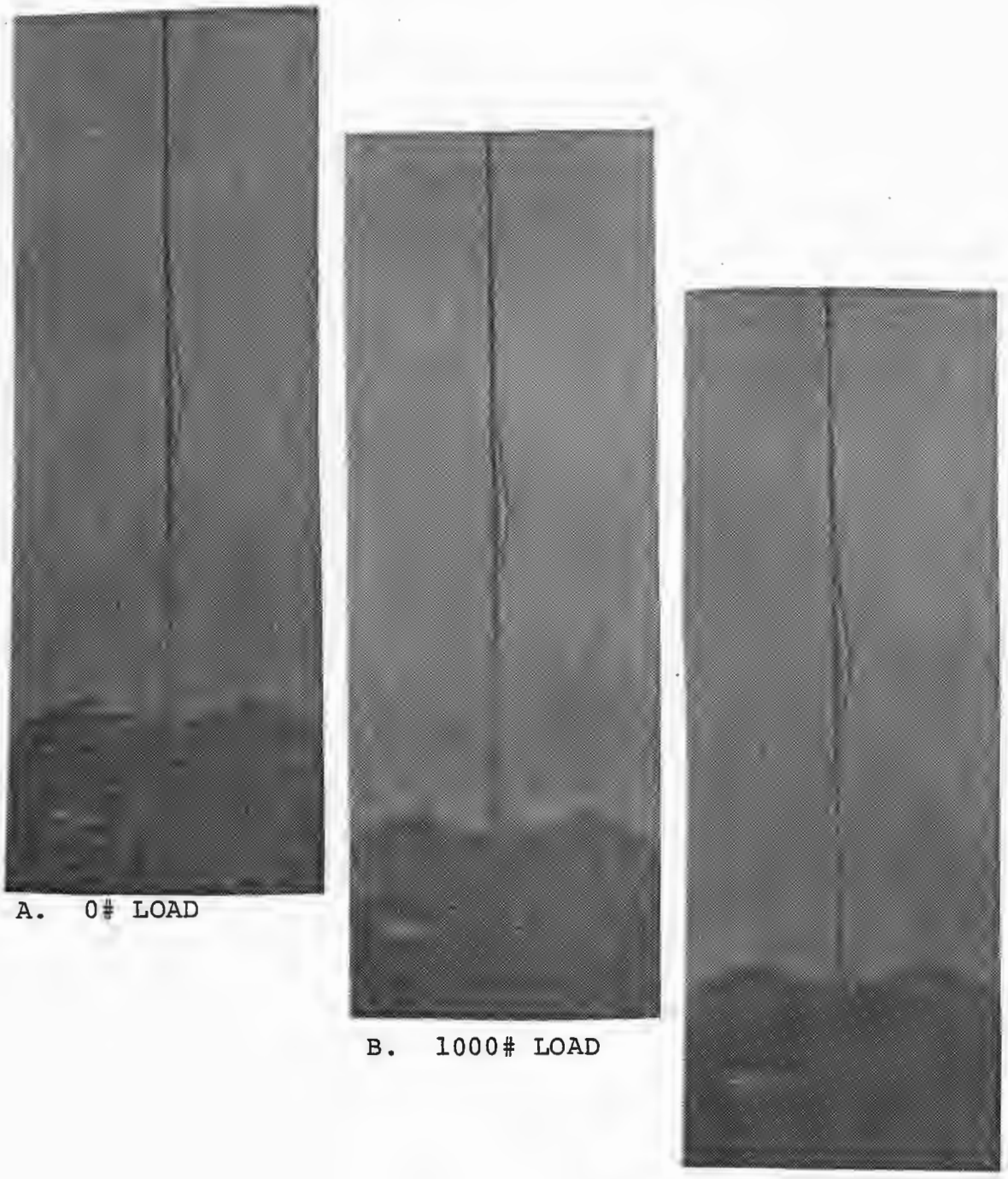

A. 0# LOAD

B. 1000# LOAD

C. 2000# LOAD

Figure 20 - TENSILE TEST LOADING-TO-FAILURE SEQUENCE

A. 3000# LOAD

B. 3500# LOAD

C. 4000# LOAD

Figure 21 - TENSILE TEST LOADING-TO-FAILURE SEQUENCE

A. 4500# LOAD

B. 5000# LOAD

C. FAILURE

Figure 22 - TENSILE TEST LOADING-TO-FAILURE SEQUENCE

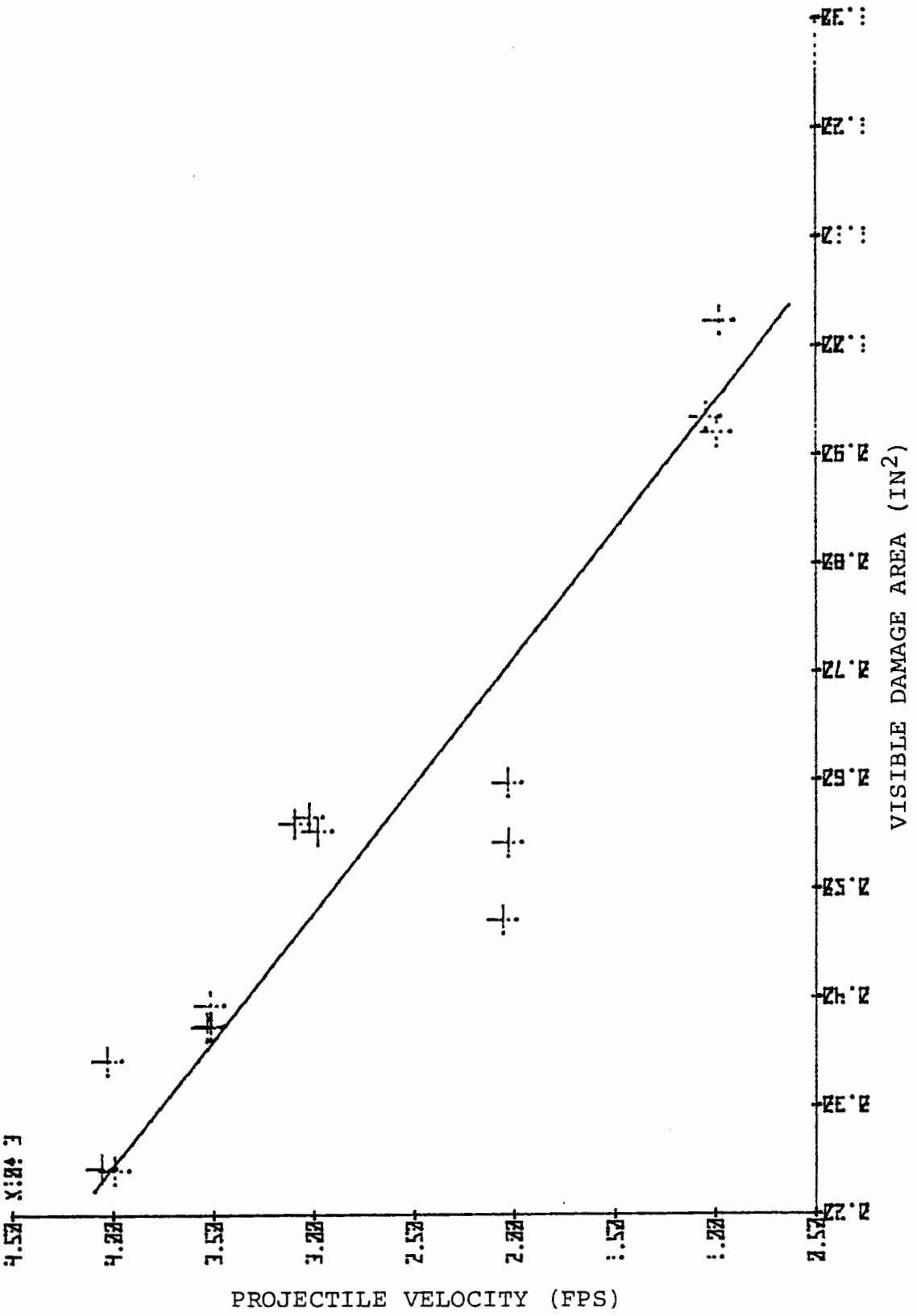

Figure 23 - VISIBLE DAMAGE AREA VS. PROJECTILE VELOCITY

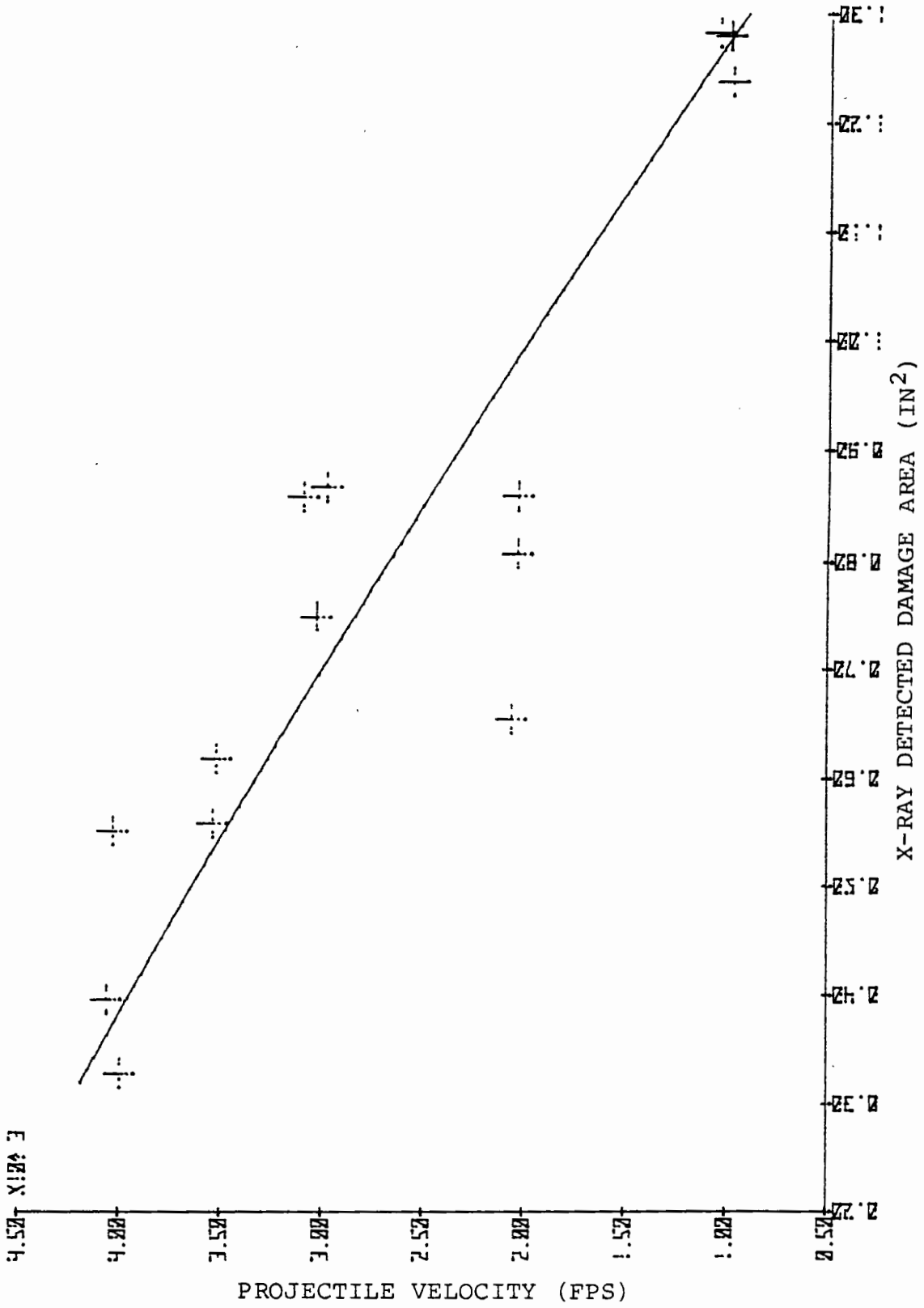

Figure 24 - X-RAY DETECTED DAMAGE AREA VS. PROJECTILE VELOCITY

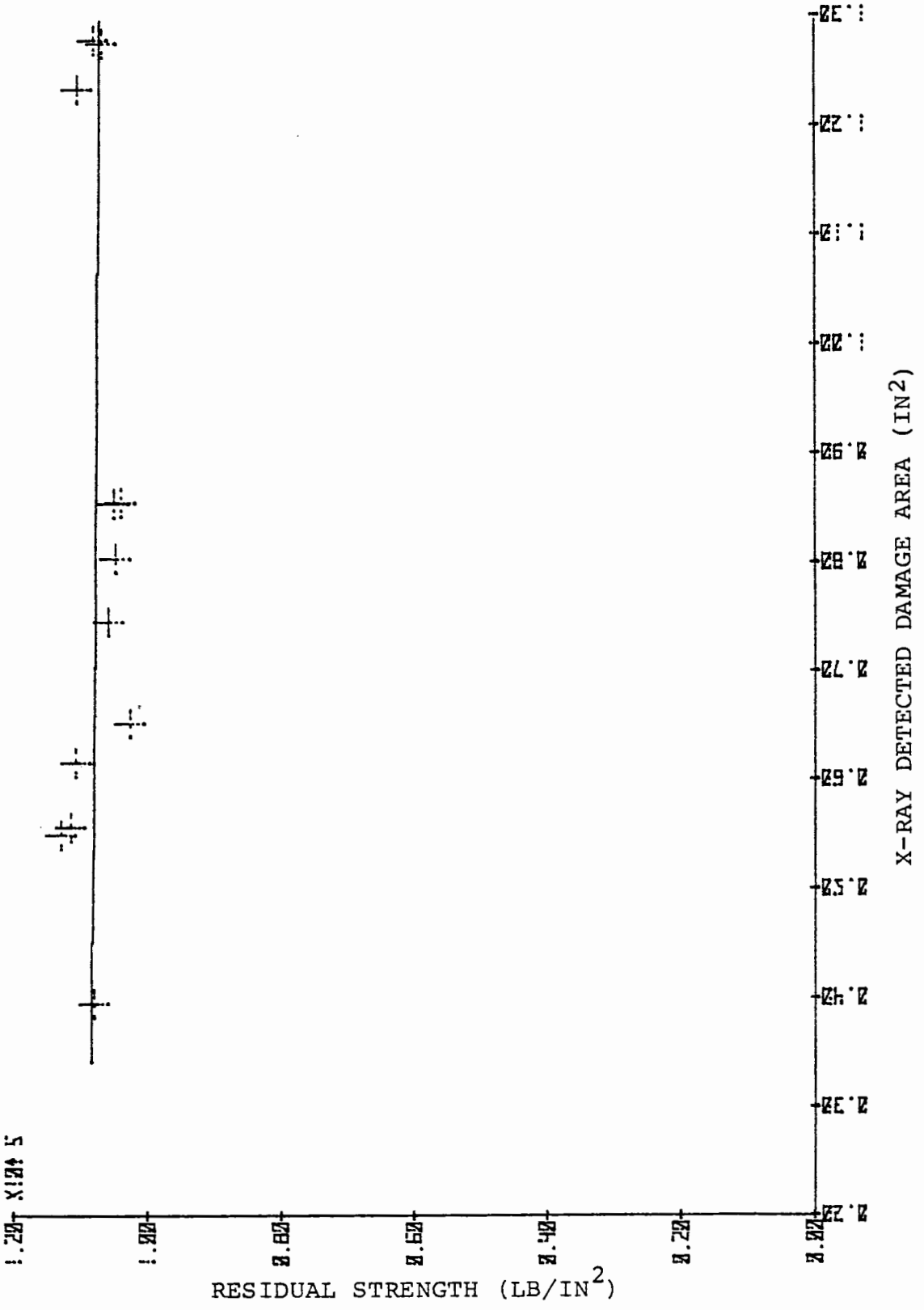

Figure 26 - X-RAY DETECTED DAMAGE AREA VS. RESIDUAL STRENGTH

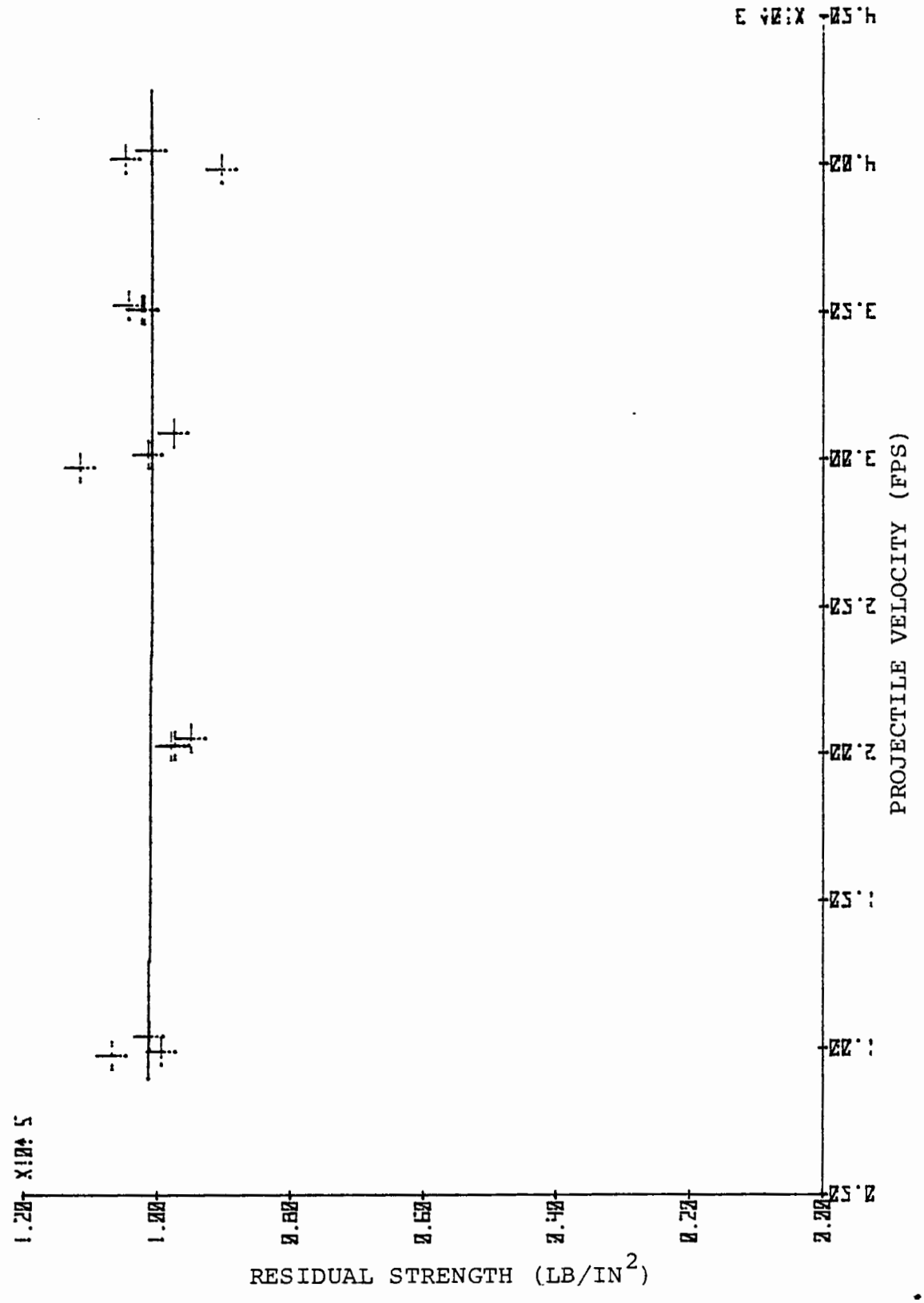

Figure 27 - RESIDUAL STRENGTH VS. PROJECTILE VELOCITY

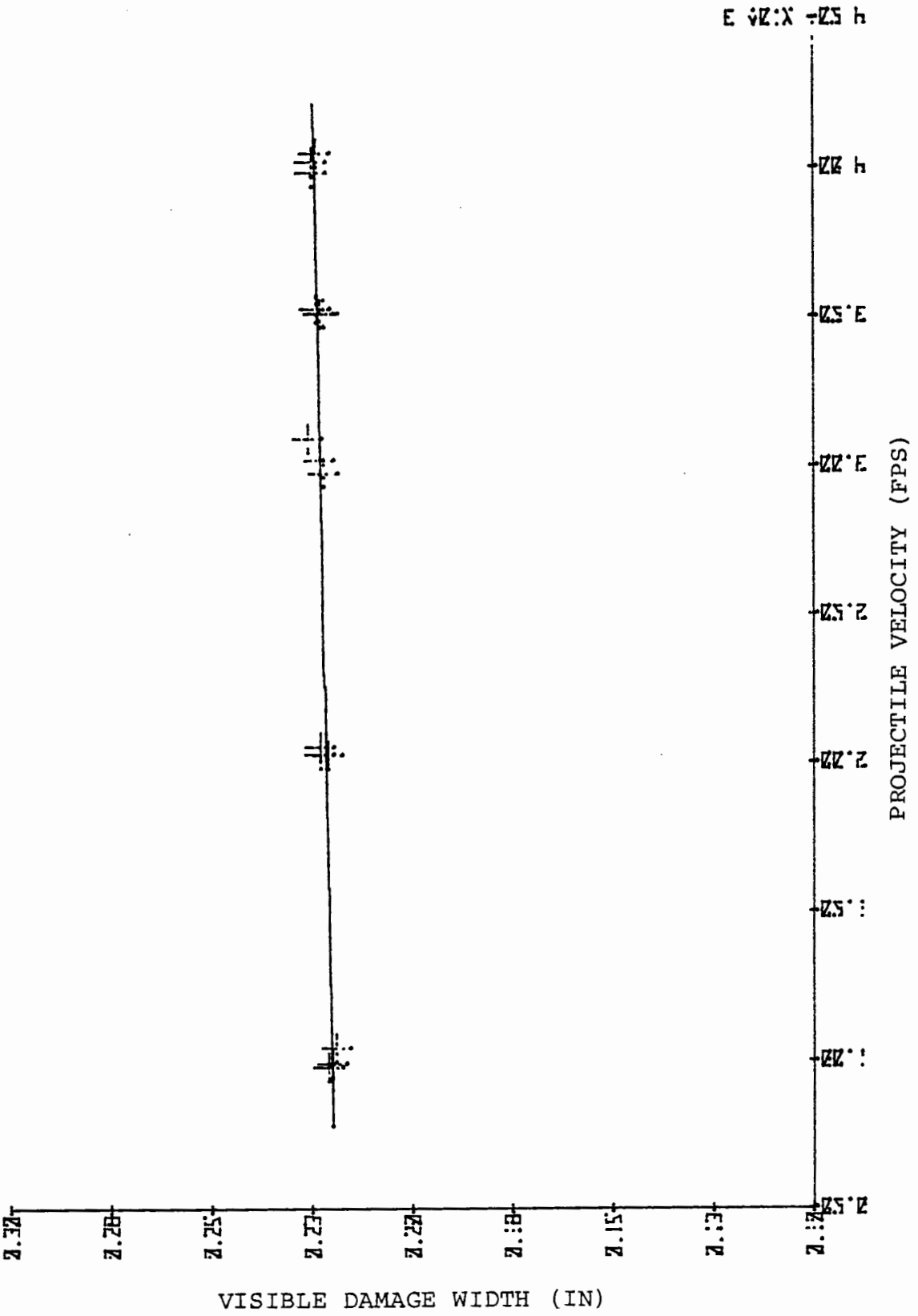

Figure 28 - PROJECTILE VELOCITY VS. VISIBLE DAMAGE WIDTH

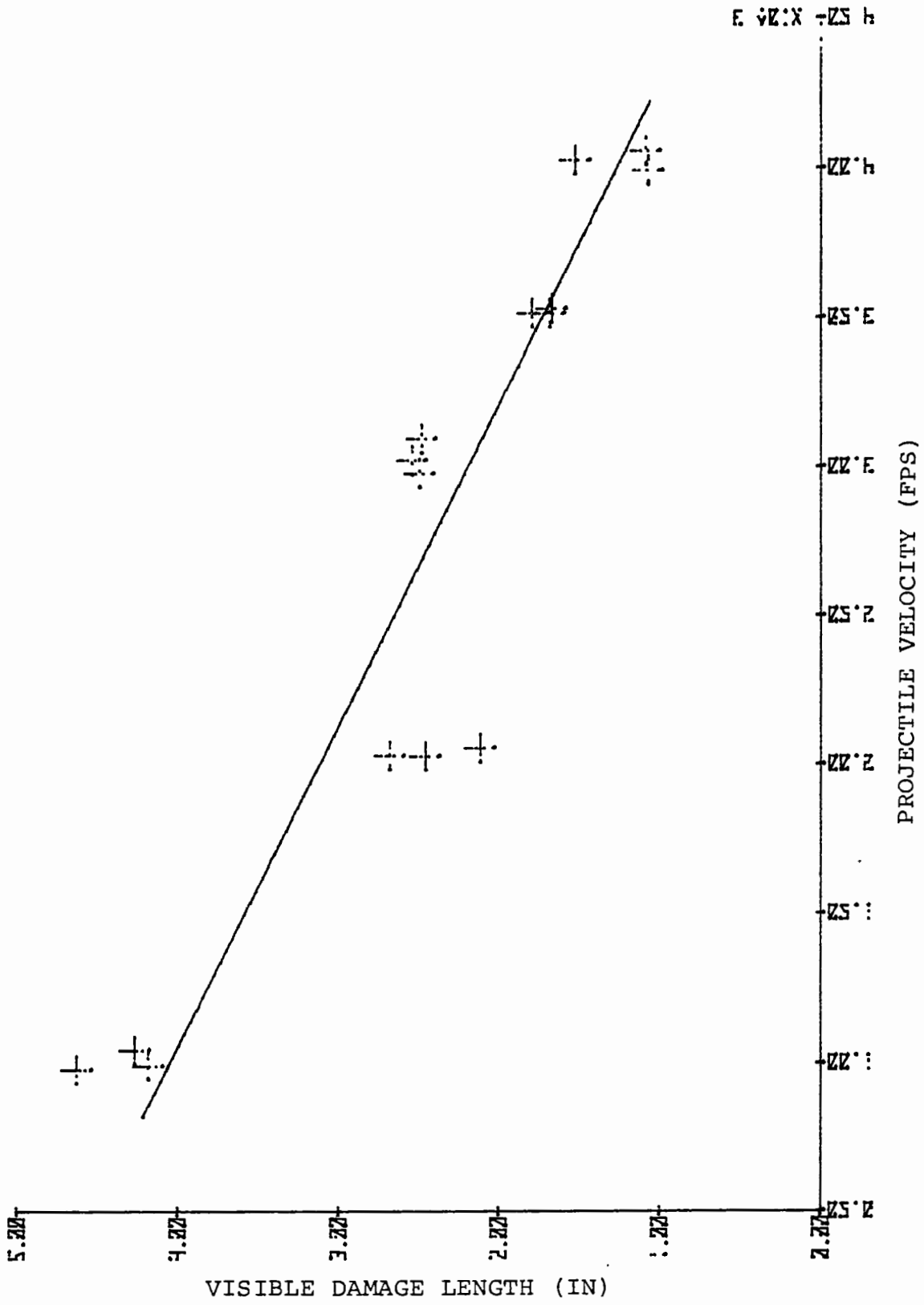

Figure 29 - PROJECTILE VELOCITY VS. VISIBLE DAMAGE LENGTH

APPENDIX A - TENSILE TEST DATA

CONTROL NUMBER	OVERALL WIDTH (IN)	WIDTH LEFT OF HOLE (IN)	WIDTH RT OF HOLE (IN)	LOAD AT FAILURE (LB)	RESIDUAL STRENGTH (LB/IN^2)
* 6-1	1.501	-	-	6535	108,844
6-2	1.502	-	-	6250	104,028
6-3	1.501	-	-	6325	105,346
**5-1	1.509	.636	.621	5250	104,415
5-2	1.505	.623	.632	5100	101,594
5-3	1.508	.623	.634	4575	90,990
6-7	1.495	.635	.639	5440	106,750
6-8	1.497	.634	.643	5075	99,354
6-9	1.492	.634	.639	5150	101,139
7-1	1.469	.606	.640	4850	97,311
7-2	1.494	.605	.666	4825	94,906
7-3	1.498	.624	.653	5000	97,886
6-4	1.502	.647	.633	5710	111,523
6-5	1.506	.637	.646	5150	101,351
6-6	1.508	.638	.644	5000	97,504

APPENDIX A (continued)

7-7	1.507	.639	.644	5350	104,248
7-8	1.502	.665	.614	5220	102,032
5-0	1.401	.500	.679	4825	102,311
7-4	1.493	.653	.615	5310	104,692
7-5	1.505	.648	.632	4625	90,332
7-6	1.503	.626	.653	5160	100,860

* Control numbers 6-1, 6-2, 6-3 were control, undamaged specimens.

** Control numbers 5-1, 5-2, 5-3 were control, drilled hole specimens.

APPENDIX B - PROJECTILE AND DAMAGE DATA

CONTROL NUMBER	PROJECTILE DATA VELOCITY/MASS	DAMAGE DATA (IN) VISUAL (XxY)	X-RAY (XxY)	RESIDUAL STRENGTH (LB/IN^2)
2-3	1014 FPS/45 GN	.220x4.550	-	-
2-2	1410 " / "	.220x3.178	-	-
2-1	2019 " / "	.219x3.092	-	-
1-1	2471 " / "	.221x1.700	-	-
1-3	3123 " / "	.219x1.452	-	-
1-2	3487 " / "	.222x1.188	-	-
2-4	3978 " / "	.221x1.378	-	-
3-2	3407 " /27.5 GN	.251x .889	.358x1.276	-
3-4	3296 " / 45 "	.220x1.167	.296x1.369	-
3-1	3348 " / 63 "	.208x1.252	.309x1.522	-
6-7	980 " / 45 GN	.221x4.629	.261x4.742	106,750
6-8	993 " / "	.220x4.184	.306x4.184	99,354
6-9	1046 " / "	.219x4.267	.297x4.320	101,139
7-1	2033 " / "	.223x2.682	.301x2.852	97,311
7-2	2058 " / "	.223x2.117	.317x2.063	94,906
7-3	2031 " / "	.221x2.456	.303x2.662	97,886

APPENDIX B (continued)

6-4	2982	" / "	.222x2.495	.336x2.578	111,523
6-5	3026	" / "	.223x2.542	.288x2.600	101,351
6-6	3098	" / "	.226x2.484	.316x2.711	97,504
7-7	3534	" / "	.224x1.670	.307x1.818	104,248
7-8	3517	" / "	.223x1.683	.323x1.914	102,032
5-0	3518	" / "	.222x1.792	-	102,311
7-4	4029	" / "	.225x1.526	.317x1.738	104,692
7-5	3994	" / "	.225x1.072	.287x1.146	90,332
7-6	4058	" / "	.224x1.087	.308x1.290	100,860

INITIAL DISTRIBUTION LIST

		No. Copies
1.	Defense Documentation Center Cameron Station Alexandria, Virginia 22314	2
2.	Library, Code 0142 Naval Postgraduate School Monterey, California 93940	2
3.	Department Chairman, Code 67 Department of Aeronautics Naval Postgraduate School Monterey, California 93940	1
4.	Asst. Prof. M. H. Bank, Code 67Bt Department of Aeronautics Naval Postgraduate School Monterey, California 93940	5
5.	LCDR George A. Eaton, USN Route 2, Box 46 White Plains, Maryland 20695	1

Thesis
E143 Eaton
c.2 Ballistic damage of
graphite-epoxy plates.
170354